

Spectroscopy of a Lithium Arc*

A.D. Naiman[†]

*Electric Propulsion and Plasma Dynamics Laboratory (EPPDyL)
Mechanical and Aerospace Engineering Department
Princeton University, Princeton, New Jersey 08544*

August 27, 2004

A lithium arc from a hollow cathode is examined using emission spectroscopy in the visible range. The goal of this observation is to determine whether spectroscopy is a useful diagnostic for low temperature lithium plasma. Using a spectroscopic diagnostic technique, the electron temperature of the single-channel hollow cathode experiment is determined to be $.4 \pm .12$ eV. The spectral line of the lowest energy transition is observed to be suppressed by two orders of magnitude from the expected intensity. Some possible explanations are proposed.

I. INTRODUCTION

This paper reports on the research conducted from June to August 2004 as part of the Program in Plasma Science and Technology Undergraduate Internship at Princeton University.

The goal of this research was to determine the feasibility of using emission spectroscopy as a plasma diagnostic to determine the electron temperature of the lithium plasma produced by various experiments at EPPDyL. Such a plasma diagnostic has been used previously at EPPDyL on other experiments, most recently in research by Markusic [1], where it was used to determine the electron temperature of an argon current sheet. This diagnostic has not, however, been applied to lithium plasma previously. Due to the nature of the technique, the applicability for use with lithium was not a given. If it can be determined that the diagnostic is feasible, however, it would provide a very useful diagnostic for future experiments, including the Lithium Lorentz Force Accelerator (LiLFA) experiment.

This paper will present the work that was accomplished in proving this technique over the summer of 2004. It will describe the experimental setup, both of the spectroscopic equipment and of the lithium plasma experiment that was observed. It will then detail the calculations that give electron temperature. The results of the experiment are presented and discussed, and some recommendations are made for future work.

II. EXPERIMENTAL SETUP

The two main components of the experimental setup are the spectroscopy instruments and the single-channel hollow cathode experiment.

A. Spectroscopy

The spectroscopy setup includes the spectrometer and all supporting equipment (grating motor controller, camera, and camera controller), PC, and optics. Figure 1 shows a schematic of the spectroscopy setup.

*Funding from Program in Plasma Science and Technology

[†]Undergraduate Research Assistant at EPPDyL.

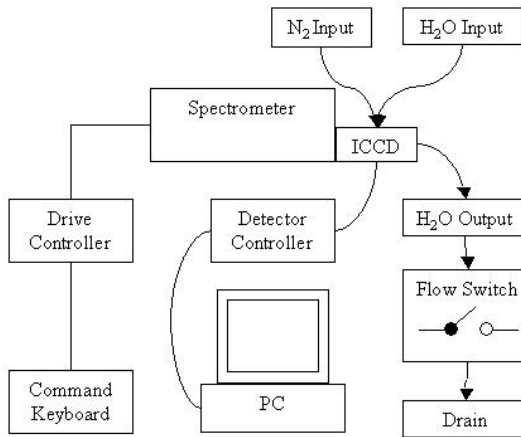


FIG. 1: Schematic of the spectroscopy setup.

1. Spectrometer

The spectrometer used in these observations is a Spex model 1702. This spectrometer features a 0.75 m focal length and a grating of 1200 grooves/mm, and is optimized for use in the visible (300 to 800 nm) range. The spectrometer grating is driven by a stepper motor, which is controlled by a Spex CD2A CompuDrive system consisting of a command keyboard and a drive controller.

2. Camera

The camera used in these observations is a Princeton Instruments model ICCD-576 image-intensified CCD camera. A Princeton Instruments ST-138 Detector Controller serves as the interface between the camera and the data collection PC. The camera is water-cooled to reduce thermal noise. In order to ensure proper cooling, the water piping is routed through a normally open water flow switch, which automatically shuts power off to the camera and controller when no water flow is detected. The CCD array is also flushed with dry nitrogen to prevent water condensation due to cooling.

3. PC

The PC used in these observations is an IBM Aptiva running Windows XP with a 450 MHz Pentium III and 512 MB RAM. This computer is also equipped with a Roper Scientific/Princeton Instruments serial buffer (PCI) card, which interfaces with the ST-138 camera controller. Camera shots are acquired using Roper Scientific/Princeton Instrument's WinSpec software package version 2.5.16.5.

4. Optics

A simple optical setup redirects light from the plasma location to the spectrometer (Figure 2). A mirror on a two-axis tilt stand and a single lens are positioned to image the plasma onto the entrance slit of the spectrometer. The internal spectrometer optics are configured such that any image falling on the entrance slit will also be in focus on the detector at the exit slit.

The additional component of the optical setup is a system that maintains a clear optical path between the detector and the plasma. When this experiment is firing, vaporized lithium enters the tank and tends to condense on the walls. Thus, after several minutes of firing, the tank window becomes completely coated

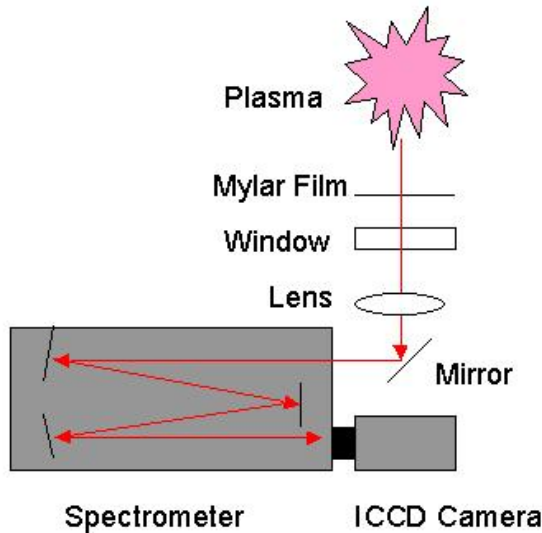


FIG. 2: Schematic of the optical setup.

with lithium (and therefore, opaque). The solution to this problem is a system that continuously rolls a Mylar film between the window and the plasma. A motor turns two rolls of the film, which are on either side of the window. As the clean film from the first roller begins to become coated with lithium, it scrolls across the window to the second roller, providing a continuously clear optical path.

B. Single-Channel Cathode Experiment

The lithium arc observed in this study was produced by the single-channel cathode experiment as part of Leonard Cassady's Ph.D. research. This experiment uses a unique feed system to push vaporized lithium through a single-channel hollow cathode. A simple ring- or bullet-shaped anode is placed approximately 3 cm from the cathode. Once an arc has been struck, the system can operate under a variety of conditions, with the mass flow of lithium between 1.0 and 6.0 mg/s and the current between 4 and 30 A.

III. CALIBRATION

The main calibration necessary for this experiment is a determination of how the optics of the setup affect the intensity of light being transmitted to the detector as a function of wavelength. To accomplish this, an Oriel 6337 Quartz-Tungsten-Halogen lamp was placed in a rod mounted fixture in the vacuum chamber at the position of the lithium arc. Camera shots of the lamp were recorded at wavelengths from 3000 Å to 8500 Å. Using the WinSpec software as well as some custom designed code (as described in Section IV B) to reduce this data, the intensity of the lamp was determined at 50 Å intervals over this range. This data was then compared to the published intensity vs. wavelength curve provided by the manufacturer of the lamp [2]. Figure 3 shows the two curves, which are combined to find an intensity calibration factor (f_i) as a function of wavelength over the visible range (Equation 1).

$$f_i = \frac{I_{published}}{I_{experimental}} \quad (1)$$

The other calibration conducted was a determination of the repeatability of intensity measurements for this particular experimental setup. As described in Section II B, a moving film passes over the window in the

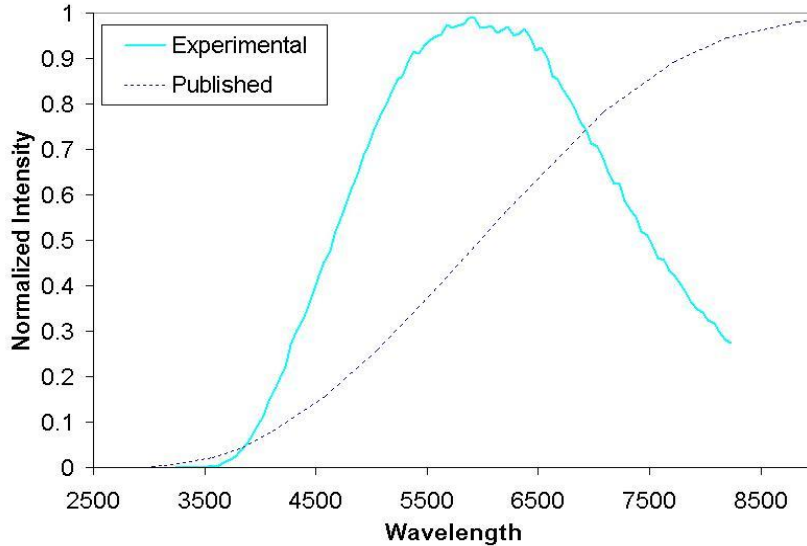


FIG. 3: The intensity calibration curves.

vacuum tank to prevent the window from being coated with lithium. This introduces an element of variability into the measurement of intensities through this window due to variations in the film. This variability was measured by taking many intensity measurements at the same wavelength for several different wavelengths throughout the visible spectrum.

With the film moving across the window, ten readings were taken at five wavelengths throughout the visible spectrum. Error was taken as the difference from the mean intensity at each wavelength. The maximum error among the fifty data points was 4.33%, while the mean error was 1.86%.

IV. EXPERIMENTAL DATA AND ANALYSIS

A. Technique

The plasma diagnostic technique used in this report was taken from the Ph. D. thesis of Thomas Markusic [1], who followed Griem [3]. The plasma is assumed to be optically thin and of depth l . The intensity of the transition from energy level m to n is given by,

$$i_{nm} = \frac{\hbar\omega_{mn}}{4\pi} A_{mn} N_m l. \quad (2)$$

Also, the plasma is assumed to be in local thermal equilibrium (LTE). Then, the population of the m^{th} energy level is given by the Boltzmann distribution,

$$\frac{N_m}{N} = \frac{g_m}{Z_a} \exp(-E_m/kT_e). \quad (3)$$

Combining (2) and (3), a linear equation of the form $y = ax + b$ can be written,

$$\ln\left(\frac{i_{mn}}{\omega_{mn} A_{mn} g_m}\right) = \frac{-1}{kT_e} E_m + \ln\left(\frac{\hbar N l}{4\pi Z_a}\right). \quad (4)$$

Using this equation as a guide, spectral line intensities can easily be used to determine electron temperature. E_m , ω_{mn} , A_{nm} , and g_m are the energy of the initial level, the frequency of the emitted radiation, the transition probability coefficient, and the degeneracy coefficient respectively. These values are known to a fair degree of accuracy for the lighter elements, including lithium [4, 5]. Thus, by measuring the intensities of the spectral lines of a plasma and using the known values,

$$y = \ln \left(\frac{i_{mn}}{\omega_{mn} A_{nm} g_m} \right) \quad (5)$$

(as in Equation 4) can be plotted against E_m . The slope of the line fit to these points is $-1/kT_e$, from which electron temperature is easily obtained.

Note that, given *absolute* intensities, the number density of the plasma could also be determined from the y-intercept of this line. Due to the problems with obtaining accurate absolute intensities, however, in most cases this is prohibitively difficult. In this study, only relative intensities were obtained, and so only the slope of this line could be used as a diagnostic.

For several different reasons, this technique is not useful for all plasmas. First of all, enough spectral lines must be present in the range over which data is being taken. Plasmas of hydrogen and helium, for example, do not emit enough lines in the visible range to give a statistically significant slope. Additionally, the observed spectral lines must have a relatively wide spread of energies. If the points are grouped too closely (i.e., on the x-axis of the plot) no line will be discernible.

B. Data Collection and Reduction

Eight different spectral lines of neutral lithium were observed over the visible spectrum in this study. Six sets of data were collected, each consisting of five shots of each of the eight lines. The WinSpec software package was used to output the intensity recorded by each pixel of the CCD camera. Each image was examined to find the brightest region and custom-written C code was used to find the arithmetic mean of the intensities in these regions. These intensities were adjusted to account for the intensity calibration and differences in exposure time, then analyzed as described above. Figure 4 shows the normalized relative intensities of the lines for a typical data set.

λ (Å)	3985.5	4132.6	4273.1	4602.9	4971.7	6103.6	6707.8	8126.4
E_m (J)	7.94E-19	7.77E-19	7.61E-19	7.28E-19	6.95E-19	6.21E-19	2.96E-19	5.40E-19
ω_{mn} (1/s)	1.20E+14	1.15E+14	1.12E+14	1.04E+14	9.60E+13	7.82E+13	7.11E+13	5.87E+13
A_{nm} (1/s)	2.50E+06	1.06E+07	4.60E+06	2.30E+07	1.01E+07	7.16E+07	3.72E+07	3.49E+07
g	2	10	2	10	2	10	6	2

TABLE I: Lithium lines seen in this study. Constant values taken from reference [4].

V. RESULTS

Table II shows the electron temperatures calculated from each of the six data sets collected. Figure 5 shows the y-coordinate (as described in IV A) plotted against energy level for a typical data set. These points lie close to the fitted line. For each of the six trials, the electron temperature was calculated to be 0.4 ± 0.12 eV. No correlation between electron temperature and either mass flow rate or current level was observed, as electron temperature did not vary outside the resolution achieved in this study.

Note that Figure 5 does not show the points consistent with all eight observed lithium lines. Figure 6 shows the eighth point, which corresponds to the spectral line that appears at 6708 Å. In all six data sets collected, the intensity of this line was two orders of magnitude lower than predicted by the linear fit of the rest of the lines. For this reason, the point was excluded in fitting a line and finding the electron temperatures listed in Table II. All six data sets can be found in Figures 7 through 12. The error bars in these plots represent the variation in intensities among the five measurements that determine each point.

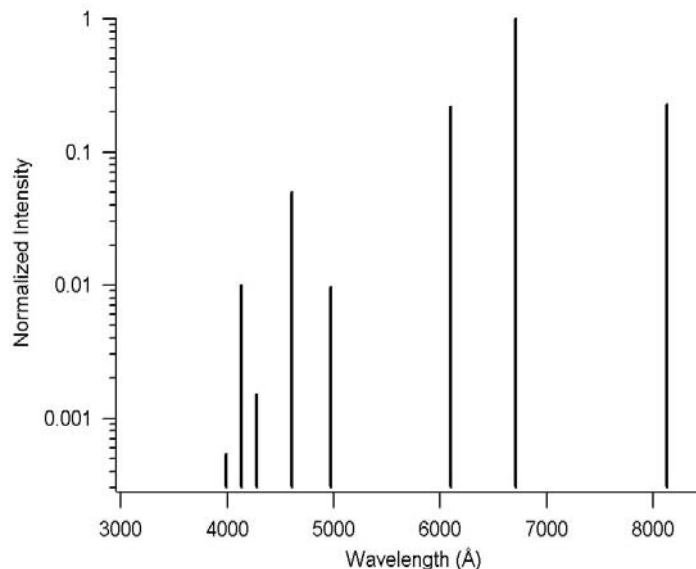


FIG. 4: Relative intensities of each line in this study shown on a log scale.

Data Set	Temperature (eV)	Current (A)	Mass Flow Rate (mg/s)
1	$.52 \pm .07$	10	6
2	$.34 \pm .03$	10	1
3	$.42 \pm .02$	20	1
4	$.41 \pm .06$	15	1
5	$.30 \pm .11$	20	1
6	$.41 \pm .02$	10	2

TABLE II: Electron temperature results for the six data sets. Error shown is based on the error in the slope of the fitted line, which in turn is based on variation in intensities among the five measurements that determine each point.

VI. DISCUSSION

The results of this study provide a useful starting point for continued spectroscopic observations of lithium plasmas. The technique presented above appears to be feasible for use as a diagnostic of such plasmas. For the most part, the observed intensities of spectral lines recorded in this experiment closely fit the expected linear distribution and indicate a reasonable electron temperature for the experiment. Thus, the analysis may be taken as correct.

The obvious problem with the results of this study, however, is the single spectral line that consistently does not fit the expected curve. Several reasons for this discrepancy are proposed, none of which affect the usefulness of the rest of the study.

The obvious starting point for explaining the diminished intensity of the 6708 Å line is an examination of the assumptions made in the analysis. The first assumption made was that the plasma was optically thin; that is, that all photons emitted by the plasma passed through the plasma without being reabsorbed. References [6–8] contain some information about the possibility of reabsorption in lithium plasmas. Given the small scale and low density of this plasma, however, this explanation seems unlikely.

The second assumption made was that the observed plasma was in LTE. References [9] and [10] as well as [3] give some guidance in verifying this assumption. Preliminary investigation of these sources indicates that there may be situations in which lower energy levels are underpopulated compared to the Boltzmann distribution while higher levels fit the LTE model. Likewise, the study conducted by Goodfellow [11] discards some lines of lower energy levels; however, no clear explanation or rationale is given for doing so. Since the

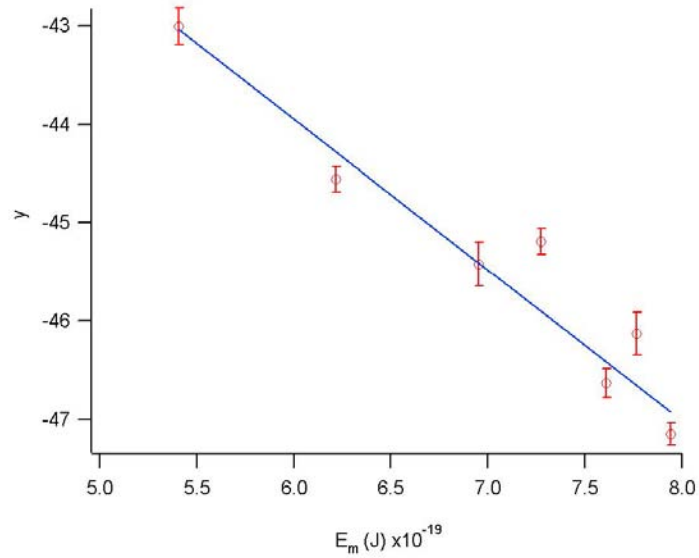


FIG. 5: Y-coordinate plotted against energy level for a typical data set with a line of best fit.

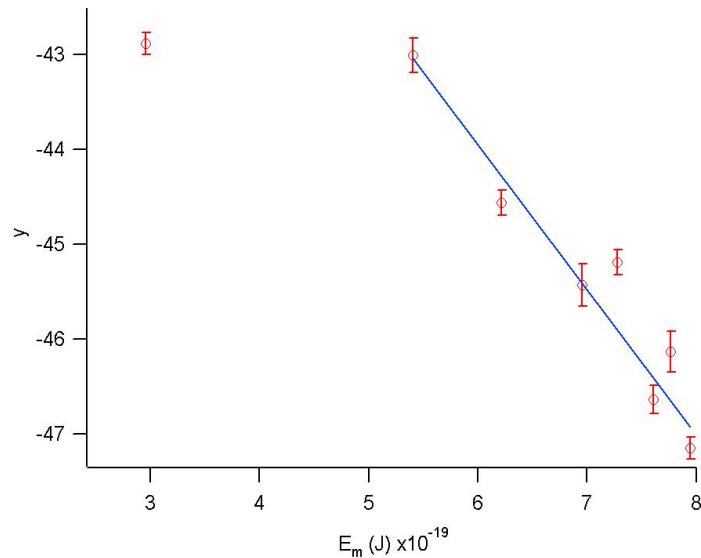


FIG. 6: The same data set with the excluded point shown.

transition that produces the 6708 Å line involves the lowest energy level of lithium, further research in this direction may provide a reasonable explanation.

Another possible explanation is the absorption or reflection of this wavelength of light by molecular lithium in the vacuum chamber. Lithium vapor is present inside the vacuum chamber during firing, and it is possible that the 6708 Å line could be obscured by this vapor. An even more likely explanation is that the small amount of lithium that condenses on the Mylar film as it rolls past the window, though appearing opaque to most wavelengths, in fact does not transmit the dimmed spectral line as readily as other wavelengths.

The reason for the dimness of this spectral line should clearly be a topic of further investigation. More research into the justification for the LTE assumption should be conducted, as other studies have noted this sort of phenomenon and have thrown away data points with little or no explanation. Additionally, the

possibility of reabsorption by lithium vapor and condensed lithium on the film should be examined further. By increasing the rate of motion of the film, the degree of condensation of lithium, and therefore opacity of the film, might be decreased.

VII. CONCLUSIONS

Emission spectroscopy appears to be a promising diagnostic for finding electron temperature. This study successfully found the temperature of the arc of a single channel cathode experiment. Similar studies should be undertaken in the future to determine electron temperature in other lithium plasma experiments, including the LiLFA experiment. Though the discrepancy of the 6708 Å line should be investigated, this method should be considered useful for lithium plasma diagnostics.

-
- [1] T.E. Markusic. *Current Sheet Canting in Pulsed Electromagnetic Accelerators*. PhD thesis, Princeton University, 2002.
 - [2] *The Book of Photon Tools*. Oriel Instruments.
 - [3] Hans R. Griem. *Plasma Spectroscopy*. McGraw-Hill Book Company, 1964.
 - [4] W.L. Wiese, M.W. Smith, and B.M. Glennon. *Atomic Transition Probabilities, Volume I: Hydrogen Through Neon*. National Bureau of Standards, 1966.
 - [5] National Institute of Standards and Technology. NIST atomic spectra database. http://physics.nist.gov/cgi-bin/AtData/main_asd.
 - [6] H. Skenderovic, T. Ban, and G. Pichler. Constriction in lithium glow discharges in a heat-pipe oven. *Optics Communications*, 161:217–222, 1999.
 - [7] D. Azinovic, S. Milosevic, and G. Pichler. Resonance 2s-2p excitation of lithium in the Li + Cd system. *Journal of Physics B*, 34:2715–2724, 2001.
 - [8] H. Skenderovic, I. Labazan, S. Milosevic, and G. Pichler. Laser-ignited glow discharge in lithium vapor. *Physical Review A*, 62, 2000.
 - [9] W. L. Wiese. Spectroscopic diagnostics of low temperature plasmas: techniques and required data. *Spectrochimica Acta Part B: Atomic Spectroscopy*, 46:831–841, 1991.
 - [10] Takashi Fujimoto and R. W. P. McWhirter. Validity criteria for local thermodynamic equilibrium in plasma spectroscopy. *Physical Review A*, 42:6588–6601, 1990.
 - [11] K.D. Goodfellow and J.E. Polk. Experimental verification of a high current cathode thermal mode. In 31st AIAA/ASME/SAE/ASEE Joint Propulsion Conference and Exhibit, San Diego, CA, July 10-12 1995.

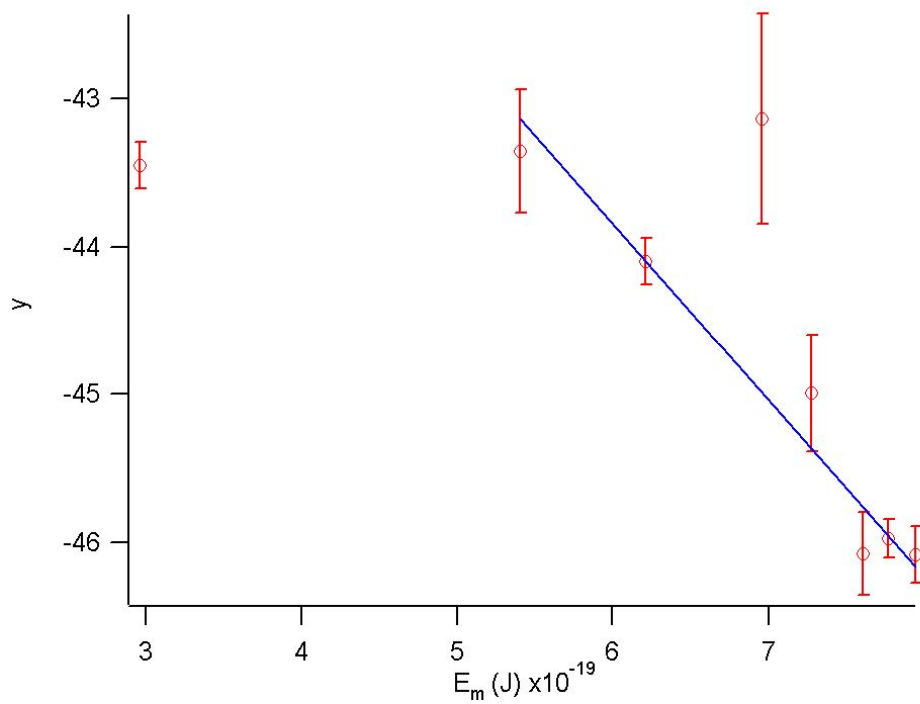


FIG. 7: Data Set 1.

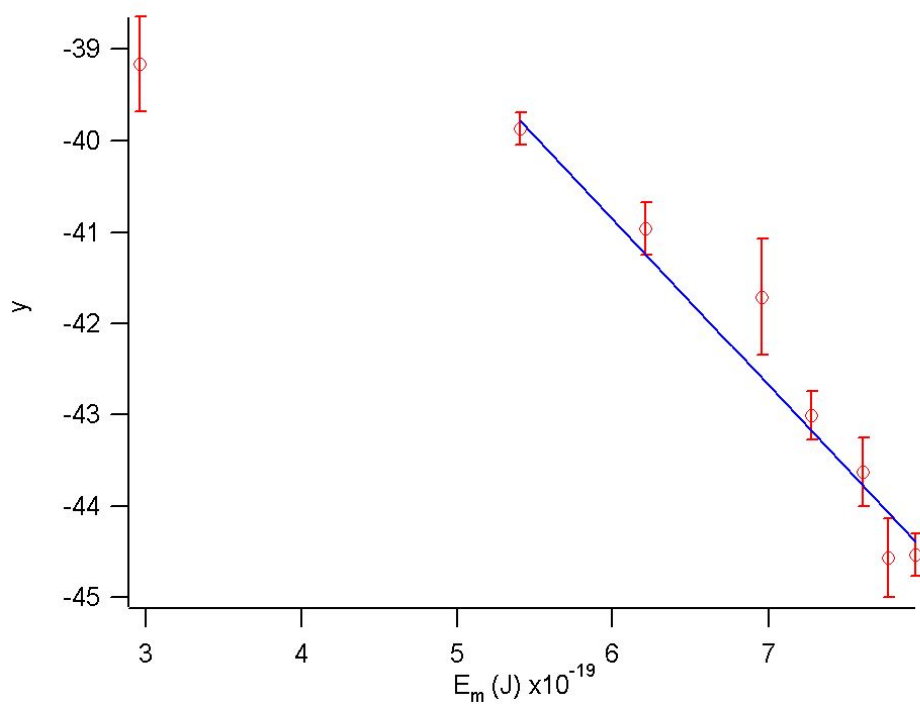


FIG. 8: Data Set 2.

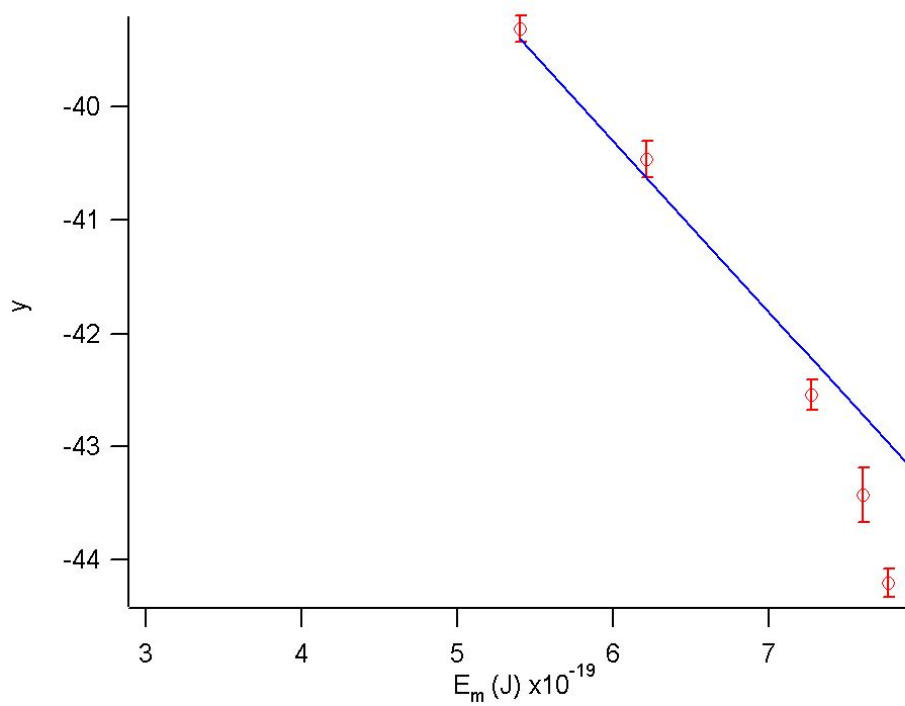


FIG. 9: Data Set 3.

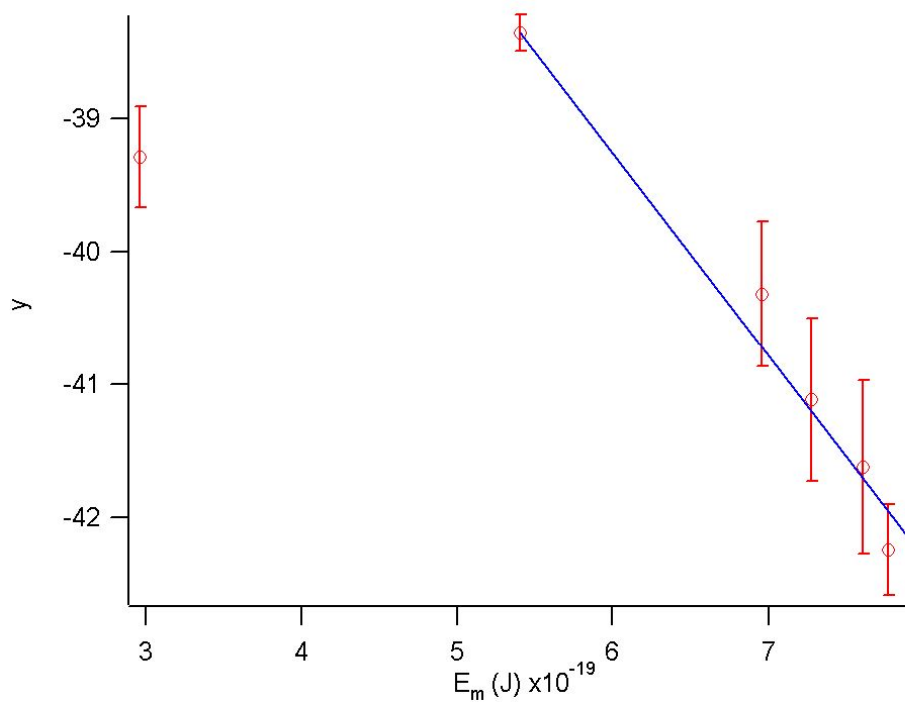


FIG. 10: Data Set 4.

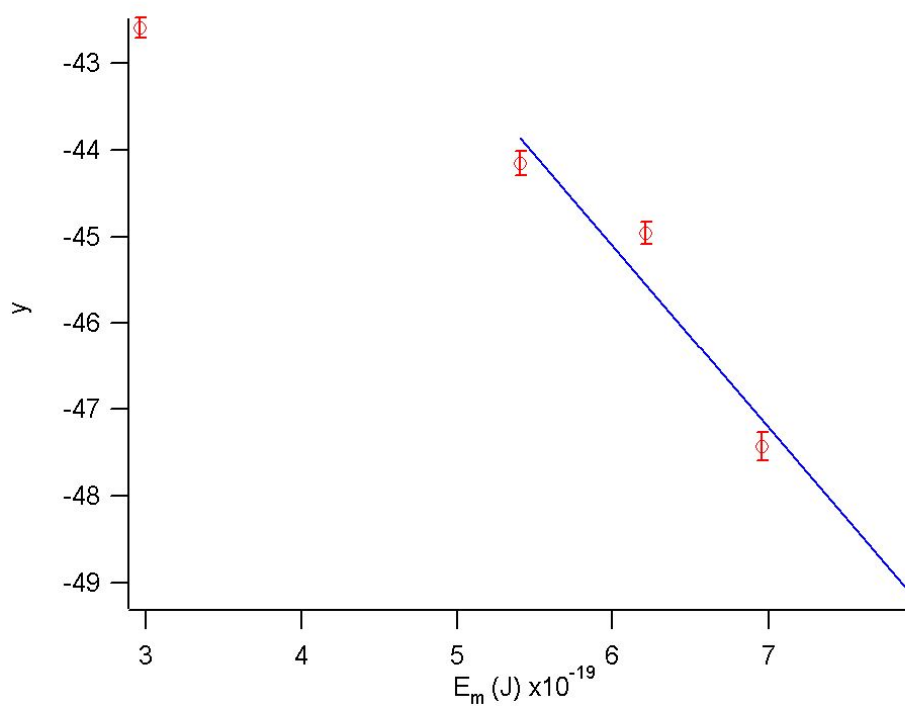


FIG. 11: Data Set 5.

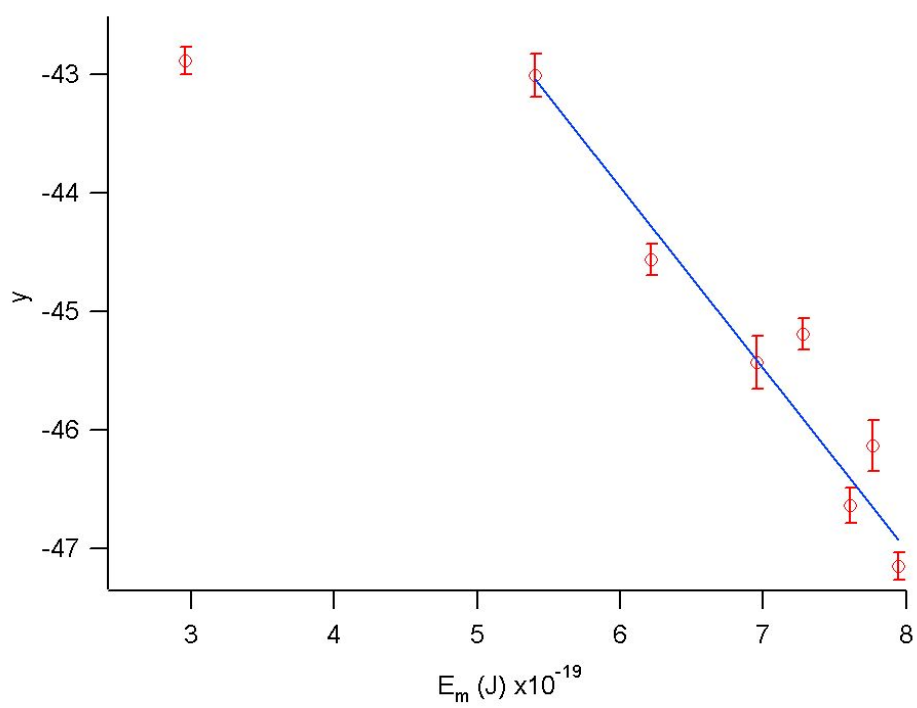


FIG. 12: Data Set 6.